Electronic Supplementary Material (ESI) for Energy & Environmental Science

Efficient CO_2 capture by humidified PEO-based polymer electrolyte membranes

By Yifan Li[a], Qingping Xin[a], Hong Wu[a], Ruili Guo[b], Zhizhang Tian[a], Ye Liu[a], Shaofei Wang[a], Guangwei He, Fusheng Pan[a] and Zhongyi Jiang[a,b*]

a. Synergetic Innovation Center of Chemical Science and Engineering (Tianjin); Key Laboratory for Green Chemical Technology of Ministry of Education, School of Chemical Engineering and Technology, Tianjin University, Tianjin 300072, China

b. Key Laboratory for Green Process of Chemical Engineering of Xinjiang Bingtuan, School of Chemistry and Chemical Engineering, Shihezi University, Xinjiang, Shihezi 832003, China

[*] Correponding author: Zhongyi Jiang, Fax: +8622 23500086; Tel: +86 22 23500086;

E-mail: zhyjiang@tju.edu.cn

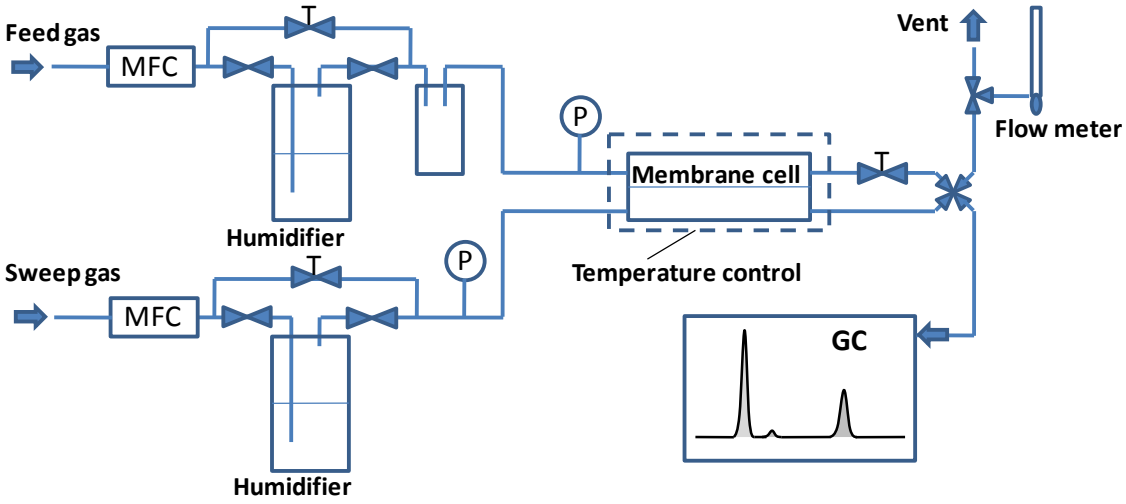

Fig. S1 Gas permeation experimental apparatus.

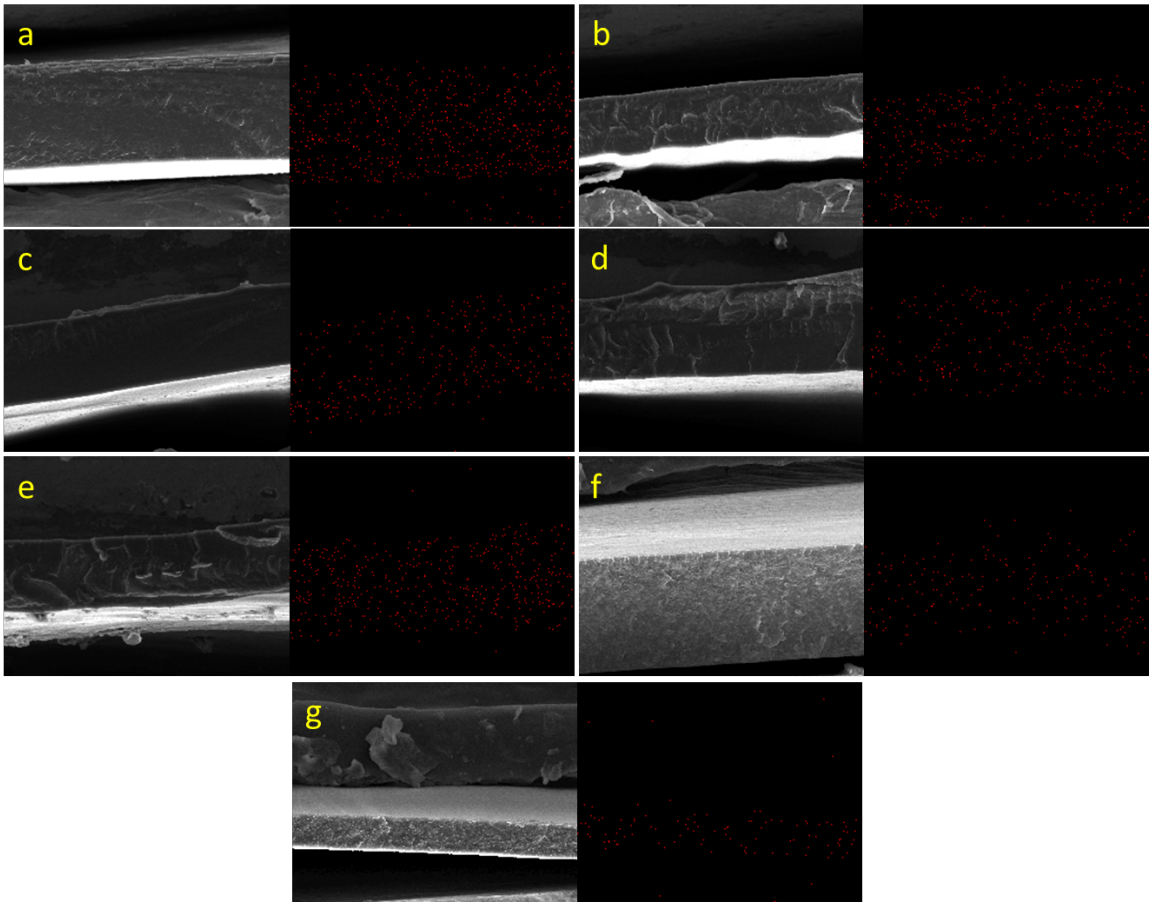

Fig. S2 Mapping-scan EDX-SEM images of (a) Pebax-NaCl(1:30); (b) Pebax-KCl(1:30); (c) Pebax-$MgCl_2$(1:30); (d) Pebax-$CaCl_2$(1:60); (e) Pebax-$CaCl_2$(1:30); (f) Pebax-$CaCl_2$(1:15); (g) Pebax-$CaCl_2$(1:7.5).

Fig. S2 shows that the salts are evenly distributed within membranes. The distribution of Li salt is not provided because Li element is too light to be probed by EDX.

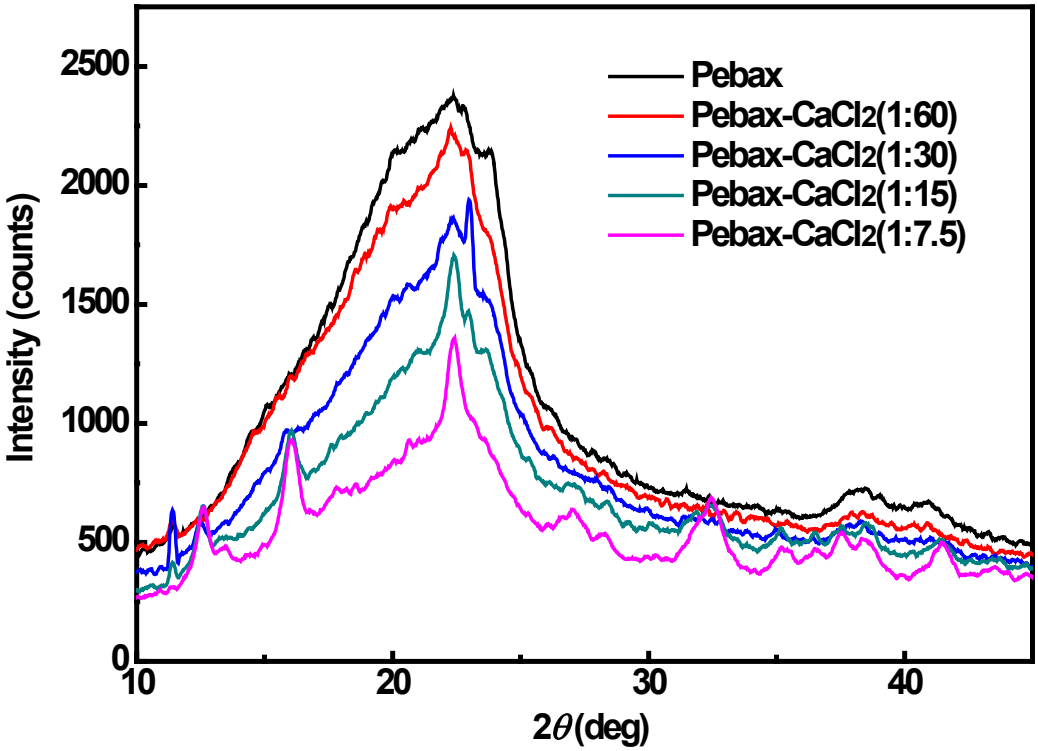

Fig. S3 WXAD curves of Pebax and $CaCl_2$-doped polyelectrolyte membranes.

The broad band with 2θ ranging from 10^o to 30^o represents the semi-crystalline structure of PA6 phase. The area covers by this band decreases with the increment of $CaCl_2$ content, demonstrating that the original crystallinity of PA6 phase can be destroyed by $CaCl_2$. For Pebax-$CaCl_2$(1:15) and Pebax-$CaCl_2$(1:7.5), the sharp peaks at 2θ=12.5^o, 15.8^o, 22.2^o, and 32.8^o can be assigned to the crystalline peaks of $CaCl_2$ crystals. The appearance of $CaCl_2$ crystals at high $CaCl_2$ content demonstrates that $CaCl_2$ has stronger tendency to self-crystallization than complex with polymer chains under such high loadings, that is, Pebax has been saturated with $CaCl_2$. For Pebax-$CaCl_2$(1:60), Pebax-$CaCl_2$(1:30) and Pebax-$CaCl_2$(1:15), new peaks at 2θ=11.4^o and 22.9^o are observed, which are different from those of $CaCl_2$ crystals. Considering the complexation between Ca^{2+} and PA6, it is reasonable to assume that a new crystalline phase comprising both PA6 and $CaCl_2$ forms at moderate $CaCl_2$ content, especially for Pebax-$CaCl_2$(1:30).

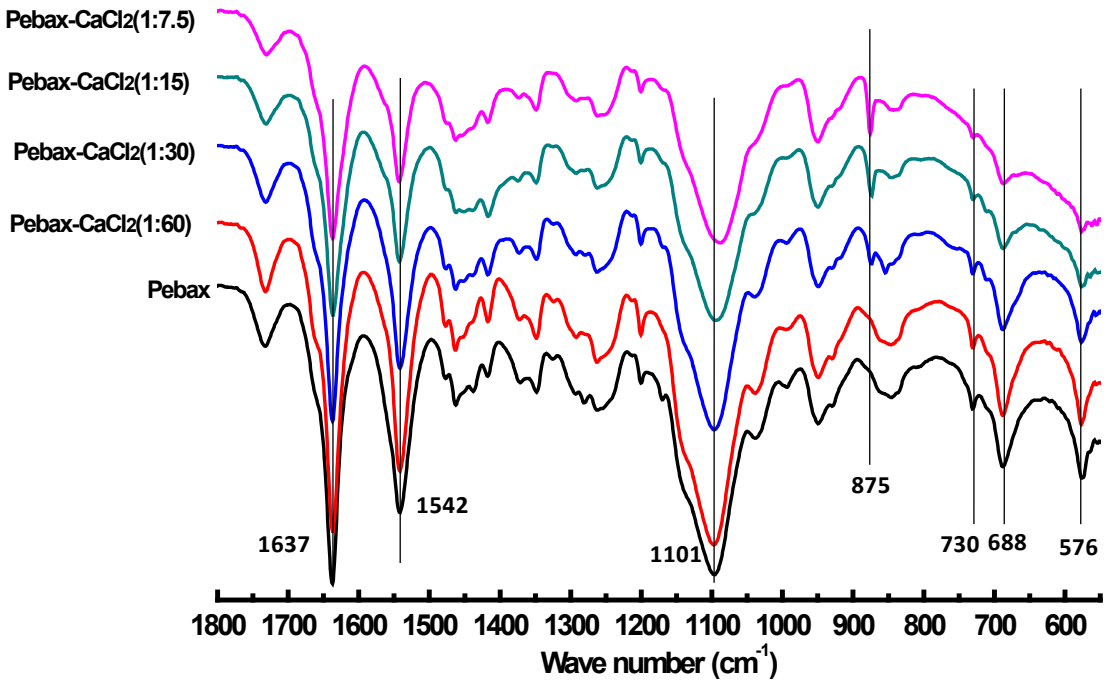

Fig. S4 FTIR curves of Pebax and $CaCl_2$-doped polyelectrolyte membranes.

The characteristic bands at 1637 and 1542 cm^{-1} were assigned to C=O stretching vibration (amide-I) and N–H deformation (amide-II) of PA6 segment, respectively. The wide and strong band near 1100 cm^{-1} was assigned to C-O stretching vibration of PEO segment. With the increase of $CaCl_2$ content, this band first remained unchanged but shifted to lower wave number for Pebax-$CaCl_2$(1:15) and Pebax-$CaCl_2$(1:7.5), implying that the strong complexation of PEO and Ca^{2+} occurred at high $CaCl_2$ content. The complexation between PA6 and Ca^{2+} was also observed by the weakened band at 730 cm^{-1}, which was assigned to plane vibration of $(–CH_2–)_4$,[1] and the other two weakened bands at 688 $cm^{-1}$and 576 cm^{-1}, which were respectively assigned to amide-IV and amide-V.[2] The strengthened band at 875 cm^{-1} for Pebax-$CaCl_2$(1:30), Pebax-$CaCl_2$(1:15), and Pebax-$CaCl_2$(1:7.5) may indicate the formation of Ca^{2+}-$(CH_2CH_2O)_n$ complex.[3]

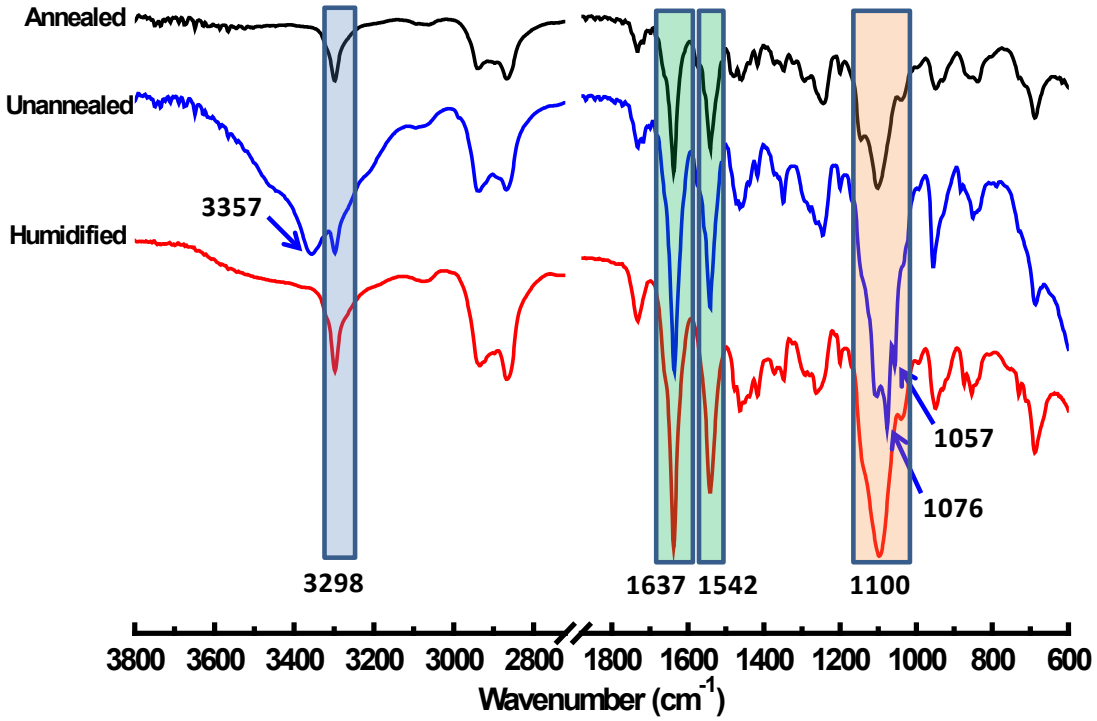

Fig. S5 FTIR curves of Pebax-$CaCl_2$(1:30) under different states.

All spectra of three samples showed the characteristic bands of N-H stretching vibration at 3298 cm^{-1}, C=O stretching vibration at 1637 cm^{-1}, and N–H deformation at 1542 cm^{-1} and for the humidified sample these characteristic bands were remarkably strengthened due to the water-induced breaking of hydrogen bonding between amide groups and the increased number of free amide groups. For the unannealed sample, a new band at 3357 cm^{-1} demonstrated the existence of large amount of O-H groups from ethanol (not water, since the band did not appear in the spectrum of the humidified sample). The new bands at 1076 cm^{-1} and 1057 cm^{-1} assigned to C-O stretching vibration of primary alcohol further supported the presence of coordinated and uncoordinated ethanol.

Table S1 Mechanical properties of dry and humidified membranes

Membrane	Dry membrane			Humidified membrane		
	Young's modulus (MPa)	Break strength (MPa)	Maximum elongation (%)	Young's modulus (MPa)	Break strength (MPa)	Maximum elongation (%)
Pebax	105	8.2	163	83	7.3	192
Pebax-LiCl(1:30)	82	8.6	123	67	7.9	144
Pebax-NaCl(1:30)	86	8.9	114	71	8.4	127
Pebax-KCl(1:30)	98	9.8	106	87	9.3	118
Pebax-$MgCl_2$(1:30)	93	9.5	108	81	8.8	125
Pebax-$CaCl_2$(1:60)	92	9.7	93	81	9.3	116
Pebax-$CaCl_2$(1:30)	101	11.5	89	95	10.7	110
Pebax-$CaCl_2$(1:15)	113	16.5	81	105	15.1	102
Pebax-$CaCl_2$(1:7.5)	129	22.0	65	115	20.4	83

The mechanical testing experiments were carried out under ambient conditions. As shown in Table S1, the addition of salt increases the break strength of Pebax membrane, especially at high salt content, indicative of the reinforcement effect of ionic crosslinking. The maximum elongation of each polymer electrolyte membrane is lower than that of Pebax membrane, demonstrating the decrease of membrane plasticity. The Young's modulus of polymer electrolyte membrane is lower than Pebax when salt:EO ratio is 1:30 or 1:60, because the crystalline region of hard block (PA6) is partially destroyed. However, for Pebax-$CaCl_2$(1:15) and Pebax-$CaCl_2$(1:15), Young's modulus is higher than Pebax, which may be ascribed to the formation of new crystalline phase, e.g. $CaCl_2$ crystals as revealed by WAXD results. On the other hand, each membrane at the humidified state shows smaller Young's modulus and larger maximum elongation, which further confirms the plasticization effect induced by water.

Table S2 Solubility and diffusivity data of Pebax and Pebax-$CaCl_2$ membranes

Membrane	S_{CO2} [a]	D_{CO2} [b]	S_{CH4} [a]	D_{CH4} [b]	S_{N2} [a]	D_{N2} [b]	S_{CO2}/S_{CH4}	D_{CO2}/D_{CH4}	S_{CO2}/S_{N2}	D_{CO2}/S_{N2}
Pebax	64.3	1.33	10.2	0.4	2.39	0.66	6.30	3.33	26.90	2.02
Pebax-$CaCl_2$(1:60)	56.6	1.17	8.3	0.35	1.97	0.54	6.82	3.34	28.73	2.17
Pebax-$CaCl_2$(1:30)	53.5	1.16	7.5	0.3	2.03	0.67	7.13	3.87	26.35	1.73
Pebax-$CaCl_2$(1:15)	41.6	0.84	7.2	0.22	2.06	0.63	5.78	3.82	20.19	1.33
Pebax-$CaCl_2$(1:7.5)	15.4	0.53	3.4	0.14	1.42	0.51	4.53	3.79	10.85	1.04

a. Solubility coefficient [cm^3 (STP)/cm^3 cmHg]$\times 10^4$;

b. Diffusivity coefficient [cm^2/s]$\times 10^6$.

The solubility and diffusivity coefficients of dry-state Pebax-$CaCl_2$ membranes were determined by the well-known "time-lag" method.[4] The experiments were conducted at 298 K and the pressure of the high-pressure side was maintained at 2 bar. It was clearly shown that at high salt loading CO_2 solubility decreases more sharply than CO_2 diffusivity, and therefore the decrease of solubility selectivity was faster than diffusivity selectivity. The drastically decreased CO_2 solubility was ascribed to the complexation between CO_2-philic EO groups and metal ions. Furthermore, at high salt loading the polymer chains became highly crosslinked by metal ions, and thus CO_2 diffusivity also decreased. The crosslinking effect guaranteed that diffusivity selectivity of CO_2/CH_4 maintained at a high value, because the separation of CO_2 and CH_4 mainly relies on size difference.

References

1 X.-H. Li, S.-D. Deng, H. Fu and G.-N. Mu, *J. Appl. Electrochem.*, 2009, **39**, 1125-1135.

2 P. Screenivasulu Reddy, T. Kobayashi, M. Abe and N. Fujii, *Eur. Polym. J.*, 2002, **38**, 521-529.

3 J.-K. Hyun, H. Dong, C. P. Rhodes, R. Frech and R. A. Wheeler, *J. Phys. Chem. B*, 2001, **105**, 3329-3337.

4 W. Yave, A. Car and K. V. Peinemann, *J. Membr. Sci.*, 2010, **350**, 124-129.